Investigational New Drugs (2019) 37:1135–1145
https://doi.org/10.1007/s10637-019-00741-3

PRECLINICAL STUDIES

GNS561, a new lysosomotropic small molecule, for the treatment of intrahepatic cholangiocarcinoma

Sonia Brun[1] · Firas Bassissi[1] · Cindy Serdjebi[1] · Marie Novello[1] · Jennifer Tracz[1] · François Autelitano[2] · Marie Guillemot[2] · Philippe Fabre[2] · Jérôme Courcambeck[1] · Christelle Ansaldi[1] · Eric Raymond[1,3] · Philipe Halfon[1]

Received: 10 January 2019 / Accepted: 1 February 2019 / Published online: 19 February 2019

Summary

Among the acquired modifications in cancer cells, changes in lysosomal phenotype and functions are well described, making lysosomes a potential target for novel therapies. Some weak base lipophilic drugs have a particular affinity towards lysosomes, taking benefits from lysosomal trapping to exert anticancer activity. Here, we have developed a new lysosomotropic small molecule, GNS561, and assessed its activity in multiple in vitro intrahepatic cholangiocarcinoma models (HuCCT1 and RBE cell lines and patient-derived cells) and in a chicken chorioallantoic membrane xenograft model. GNS561 significantly reduced cell viability in two intrahepatic cholangiocarcinoma cell lines (IC_{50} of 1.5 ± 0.2 μM in HuCCT1 and IC_{50} of 1.7 ± 0.1 μM in RBE cells) and induced apoptosis as measured by caspases activation. We confirmed that GNS561-mediated cell death was related to its lysosomotropic properties. GNS561 induced lysosomal dysregulation as proven by inhibition of late-stage autophagy and induction of a dose-dependent build-up of enlarged lysosomes. In patient-derived cells, GNS561 was more potent than cisplatin and gemcitabine in 2/5 and 1/5 of the patient-derived cells models, respectively. Moreover, in these models, GNS561 was potent in models with low sensitivity to gemcitabine. GNS561 was also efficient in vivo against a human intrahepatic cholangiocarcinoma cell line in a chicken chorioallantoic membrane xenograft model, with a good tolerance at doses high enough to induce an antitumor effect in this model. In summary, GNS561 is a new lysosomotropic agent, with an anticancer activity against intrahepatic cholangiocarcinoma. Further investigations are currently ongoing to fully elucidate its mechanism of action.

Keywords GNS561 · Cholangiocarcinoma · Anticancer · Lysosome · Apoptosis

Introduction

Primary liver cancer is a worldwide leading cause of cancer-related death, standing at the fourth position [1]. Among primary liver cancers, cholangiocarcinoma (CCA) accounts for nearly 10%, behind hepatocellular carcinoma [2]. Although CCA is recognized by the FDA (Food and Drug Administration) as an orphan disease, usually defined as a condition that affects fewer than 200,000 people nationwide, the incidence of CCA is increasing in several countries and in Asia, where the main identified risk factors are hepatitis B and C infections [3–5].

Intrahepatic CCA (iCCA) is defined as a particular biliary duct cancer located proximally to the second-degree bile ducts [6]. Curative treatment of iCCA relies on surgery, but tumor resection is possible in only 30–40% of patients. Due to the lack of specific symptoms, iCCA is often diagnosed at late stages in most patients [7], when surgery is no longer a therapeutic option [8].

To date, the recommended first-line therapy remains gemcitabine-platinum combinations (ABC-02 trial) [3], with modest efficacy (median progression-free survival of 8.0 months and median overall survival of 11.7 months). Numerous attempts have been made to replace this combination but most investigated drugs or combinations failed to significantly improve survival in first- and second-line

Electronic supplementary material The online version of this article (https://doi.org/10.1007/s10637-019-00741-3) contains supplementary material, which is available to authorized users.

✉ Sonia Brun
s.brun@genosciencepharma.com

[1] Genoscience Pharma, 10 Rue d'Iéna, Marseille, France

[2] Biomarker Discovery Department, Evotec SAS, 195 Route d'Espagne – BP13669, Toulouse, France

[3] Department of Oncology, Hôpital Paris Saint Joseph, 185 Rue Raymond Losserand, Paris, France

settings [7–9]. Immunotherapies and molecular targeted approaches are thought to be quite promising in CCA [10]. For instance, drugs targeting IDH1/2 (isocitrate dehydrogenase) mutations and FGFR2 (fibroblast growth factor receptor-2) protein fusions offer great promise in iCCA [11]. Derazatinib (ArQule, Inc., USA), an FGFR2 inhibitor, and Ivodesinib (Agios Pharmaceutical, USA), an IDH1/2 inhibitor, are currently being evaluated in Phase 3 clinical trials as second-line therapy in advanced iCCA. However, IDH1/2 mutations and FGFR2 aberration mutations are only reported in 14% and 13–20% of patients with iCCA, respectively.

Because of their high metabolic rates, rapidly dividing and invasive cancer cells are highly dependent on lysosomal functions [12–14]. Lysosomes contain hydrolytic enzymes that play a major role in the degradation of intracellular macromolecules and catabolic (such as autophagy and micropinocytosis) and anabolic growth [15–17]. Lysosomes are important in the malignant process [18] and are required in tumor cells for cellular adhesion, motility and signaling, exocytosis, angiogenesis and overall survival, growth, aggressiveness and metastasis [19–23]. Thus, cancer cell lysosomes tend to become hyperactive when fulfilling the needs of the challenging tumor microenvironment [12, 21, 22, 24]. This busy lysosomal behavior is associated with increased lysosomal biogenesis, volume and protease activity and is accompanied by changes in the composition and the cellular distribution of the lysosomal compartment [12, 19, 25–32]. However, such alterations that confer phenotypic advantages to tumors can markedly lead to weaker lysosomal membranes in cancer cells compared to noncancerous cells, resulting in sensitization to lysosomal membrane permeabilization (LMP) and, eventually, to cell death [12, 14, 29, 33–35]. Therefore, lysosomes seem to be a potential target organelle for the chemotherapy of tumors. Targeting lysosomes not only triggers apoptotic and lysosomal cell death pathways but also inhibits cytoprotective autophagy [22, 30, 31, 36–38], a pathway that is known to be important in iCCA development, progression and invasion [39–42]. Hence, a promising strategy for anticancer therapy in iCCA can be to target lysosomes.

Based on evidence showing that chloroquine and its derivatives may induce lysosome-mediated cell death, many researchers have focused on chloroquine effects in cancer therapy [35, 43–46]. Over 40 single agent and combination clinical trials have been reported using several chloroquine derivatives [47–49]. However, these drugs failed in demonstrating sufficient efficacy at therapeutic levels, limited by their modest potency and the frequently induced side effects, such as ocular toxicity and irreversible retinopathy [30, 31, 50–52].

In this context, we herein discovered a novel lysosomotropic small molecule, GNS561. We investigated the antitumor activity of GNS561 in human iCCA cell lines and patient-derived cells, as well as its potential to inhibit tumor growth in a chicken chorioallantoic membrane (CAM) xenograft model. Due to its physicochemical characteristics, we investigated if GNS561-induced cell death was mediated by its lysosomotropic properties.

Based on this study, we provide a rationale for targeting lysosomes as a promising therapeutic strategy in iCCA in human clinical trials.

Materials and methods

Chemicals

Bafilomycin A1 (Baf) and ammonium chloride (NH_4Cl) were obtained from Sigma-Aldrich (St Louis, MO, USA). Cisplatin and gemcitabine were supplied by Santa Cruz Biotechnology (Dallas, TX, USA).

Cell culture

Two iCCA cell lines, HuCCT1 and RBE, were obtained from JCRB (Japanese Cancer Research Resources Bank) Cell Bank (Osaka, Ibaraki, Japan) and RIKEN Cell Bank (Tsukuba, Ibaraki, Japan), respectively. The cells were cultured using Roswell Park Memorial Institute (RPMI) medium supplemented with 1% penicillin-streptomycin and 10% fetal bovine serum. Cells were maintained at 37 °C in the presence of 5% CO_2 and 95% air in a humidified incubator.

Cell viability assay

Cell viability was assessed using the CellTiter Glo® Luminescent Cell Viability Assay following the manufacturer's protocol (Promega, Madison, WI, USA). Briefly, cells were plated in 96-well tissue culture plates (3000 cells per well) in 90 μL of medium. Twenty-four hours after plating, cells were treated with 10 μL of increasing concentrations of drug (GNS561, gemcitabine or cisplatin) or vehicle and incubated for 72 h. At the end of treatment, 100 μL of CellTiter Glo solution was added to each well; cells were shaken and then incubated at room temperature for 10 min to allow stabilization of the luminescent signal. The luminescence was recorded using an Infinite F200 Pro plate reader (Tecan, Männedorf, Switzerland) and cell viability was expressed as a percentage of the values obtained from the negative control cells (cells treated with vehicle). The half-maximal inhibitory concentration (IC_{50}) was evaluated using a nonlinear regression curve in GraphPad Prism 7 (GraphPad Software, La Jolla, CA, USA). For each cell line, at least six concentrations were tested in triplicate. Mean IC_{50} was calculated as the average of three independent experiments.

Caspases 3/7 activity assay

Caspases 3/7 activity was measured using Caspase-Glo® 3/7 Assay following the manufacturer's protocol (Promega). Briefly, cells were plated in 96-well tissue culture plates (3000 cells per well) in 90 μL of medium. Twenty-four hours after plating, cells were treated with 10 μL of 10X GNS561 solution (final concentrations:1, 2, 3, 4 and 6 μM for HuCCT1 and 1.8, 3.6, 5.4 and 7.2 μM for RBE) or vehicle (i.e., medium with DMSO) and incubated for 24 h. At the end of treatment, 100 μL of Caspase-Glo 3/7 reagent were added to each well and incubated for 1 h at room temperature. Then, luminescence was measured by an Infinite F200 Pro plate reader. Fold-increased activation of caspases 3/7 was determined by comparing the luminescence in the treated groups to the luminescence observed in the negative control wells (wells treated by vehicle), with the luminescence of blank wells subtracted. At each time point, in parallel with caspases 3/7 activation, cell viability was also investigated using CellTiter-Glo® Luminescent Cell Viability Assay. Each concentration of GNS561 was tested in duplicate in at least three independent experiments.

Lysosomotropism-mediated death study

Briefly, RBE cells were plated in 96-well tissue culture plates (3000 cells per well) in 80 μL of medium. Twenty-four hours after plating, cells were pretreated with 10 μL of Baf (100 and 200 nM) or NH_4Cl (10 and 20 mM) for 2 h and then treated with increasing concentrations of GNS561 (final concentrations: 1.8, 3.6, 5.4, 7.2 and 9 μM) or vehicle (i.e., medium with DMSO) and incubated for 24 h. At the end of treatment, cell viability was assessed using the CellTiter Glo® Luminescent Cell Viability Assay following the manufacturer's protocol. Cell viability was expressed as a percentage of the values obtained from the negative control cells (cells treated with vehicle). Each condition was tested in triplicate and at least three independent experiments were performed.

Autophagy assay

RBE cells were plated in 6-well tissue culture plates (125,000 cells per well) in 1.8 mL of medium. Twenty-four hours after plating, cells were treated with 200 μL of 10X GNS561 solution (final concentrations: 0.9, 1.8 and 3.6 μM) for 24 h. Treatment with vehicle (i.e., medium with DMSO) was used as a baseline for autophagic flux control. In specified conditions, Baf was added for the last 2 h of treatment (100 nM). Immunoblot analysis of light chain 3 phosphatidylethanolamine conjugate (LC3-II) and glyceraldehyde-3-phosphate dehydrogenase (GAPDH) were performed in parallel. In brief, cells were lysed with Mammalian Cell Lysis Buffer (GE Healthcare, Chicago, IL). A cOmplete™ Protease Inhibitor Cocktail (Sigma-Aldrich) was added extemporaneously to the lysis buffer. Ten micrograms of protein from each sample were separated on a 15% SDS-PAGE gel, transferred to a PVDF (polyvinylidene difluoride) membrane, and blotted with an antibody against LC3 (Sigma-Aldrich). Immunoblotting with an antibody against GAPDH (Abnova, Taipei, Neihu, Taïwan) was used as a loading control. The antibody dilutions used were as follows: anti-LC3 1:3000 and anti-GAPDH 1:5000. The LC3-II and GAPDH signal were quantified using ImageJ software (NIH, USA). The normalized LC3-II levels (Norm LC3-II) and the autophagic flux were calculated, respectively, as LC3-II signal/GAPDH signal ratios and as the ratio between Norm LC3-II levels with Baf and Norm LC3-II levels without Baf. The autophagic flux was expressed in arbitrary units. Three independent experiments were performed.

Lysosomes detection

The detection of lysosomes was performed using the LysoTracker Red DND-99 probe (LysoTracker) (Invitrogen, Carlsbad, CA, USA) under fluorescence microscopy following the manufacturer's instructions. RBE cells were plated in a 4-well chamber slide at a density of 300,000 cells per well. Twenty-four hours after plating, cells were treated with GNS561 at different concentrations (final concentrations: 5 and 10 μM) or vehicle for 30 min. Following treatment, the medium was replaced with fresh medium containing 75 nM LysoTracker. After incubation for another 30 min, the medium was removed and cells were washed 3 times with warmed HBSS (Hanks Balanced Salt Solution) and viewed on a Zeiss Axiovert200M Confocal spinning disk microscope. Lysosomes were detected as a red color (excitation 642 nm and emission 655 nm). For each treatment, three large microscopy images showing multiple cells (> 30) and three high-power photomicrographs showing one cell per field were collected.

Microscopy and image analysis

Images were acquired on an Axiovert200M Zeiss microscope using a CSU-W1 Yokogawa confocal unit. This microscope was equipped with an alpha plan Apochromat X100 oil immersion objective (NA 1.46). Images were captured with an EMCCD (Electron- Multiplying Charge Coupled Device) ProEM 1024X1024 camera (Princeton Instruments, Trenton, NJ, USA). Images were acquired with Metamorph software (Molecular Devices, San Jose, CA, USA). For large images containing several cells, the integrated morphometry analysis function in the Metamorph software was used to measure the total intensity. For single cell images, the granulometry analysis application module of Metamorph software was applied to measure their intensity. Data representing the mean of three large images or of three single cell images per condition were plotted as a percentage of vehicle + SD using GraphPad Prism 7.

Ex vivo 3D methylcellulose assay

Patient-derived xenograft (PDX) tumor-bearing animals were maintained at Crownbio HuPrime animal facility (Crown Bioscience Inc., Taicang, China). To collect PDX cells, xenograft tumors were harvested when tumor volumes reached 500–800 mm^3, minced and dissociated in collagenase (Invitrogen, Carlsbad, CA, USA) working solutions at 37 °C for 1–2 h. After removal of red blood cells using red blood cell lysis buffer, tumor cells were washed with PBS (Phosphate Buffered Saline) and resuspended in cryopreservation medium at a density of approximately 3–5 × 10^6 cells/ml and banked in a liquid nitrogen tank. An ex vivo 3D methylcellulose assay was performed using five cell models (CC6205, CC6279, CC6625, CC6638 and CC6658). Cell viability was counted using trypan blue. To carry out the ex vivo 3D assay using cryopreserved PDX cells, frozen vials of dissociated PDX cells were revived, resuspended in 0.65% methylcellulose (final concentration), loaded into 96-well plates, and cultured overnight in a 37 °C incubator with a supply of 5% CO_2. Test compounds (GNS561, gemcitabine and cisplatin) were then added in 9 concentrations in triplicate. After a 7-day incubation, cell viability was measured by CellTiter Glo® Luminescent Cell Viability Assay. Results are plotted using GraphPad Prism 7 to determine IC_{50} values.

Chick embryo tumor growth assay

In vivo tumor proliferation of the HuCCT1 cell line was assessed by the chick embryo tumor growth assay (Inovotion, Grenoble, France), as previously described [53–56]. Briefly, fertilized white leghorn eggs were incubated at 37.5 °C with 50% relative humidity for 9 days. At day 9, the CAM was dropped by drilling a small hole through the eggshell into the air sac and a 1 cm^2 window was cut in the eggshell above the CAM. Cultured HuCCT1 (at 85% confluency) were detached by trypsinization, washed with complete medium and suspended in PBS. An inoculum of 1 × 10^6 cells was added directly onto the CAM of each egg (D9). After graft, the eggs were individually checked every day. Eggs were then randomized in 4 groups of 21 eggs to get a sufficient number of surviving embryos at the end of the experiments. One day later, tumors began to be detectable. They were then treated every 2 days over the next 8 days (D11, D13, D15, D17), by dropping 100 μL of either GNS561 at two different doses (75 and 150 μM), gemcitabine (150 μM) or vehicle (0.3% DMSO in PBS) onto the tumor. The dropwise addition of a solution onto the large tumor area that depressed the CAM surface was found to be a suitable method that avoided leakage and dispersion of the compounds. Then, the windows were sealed with adhesive tape and the eggs were returned to the incubator. At day 18 (D18), the upper portion of the CAM was removed from each egg, washed in PBS and then directly transferred to paraformaldehyde (fixation for 48 h) and weighed. Finally, treatment toxicity was evaluated by scoring the number of dead embryos and looking for morphological or functional abnormalities in the surviving embryos.

Statistical analysis

All statistical analyses were performed using GraphPad Prism 7. The comparisons of means were calculated using one-way ANOVA with either Dunnett's or Dunn's post hoc analysis. Statistical significance was defined as p-values < 0.05.

Results

GNS561 significantly reduces cell viability of iCCA cells by induction of apoptosis

We first investigated cell viability using various concentrations of GNS561 in human iCCA cell lines. As shown in Fig. S1 and Table 1, treatment with GNS561 for 72 h reduced cell viability with an IC_{50} of 1.5 ± 0.2 μM in HuCCT1 and an IC_{50} of 1.7 ± 0.1 μM in RBE cells. We also compared GNS561 activity to that of two reference control drugs frequently used in iCCA, gemcitabine and cisplatin. GNS561 was more effective than gemcitabine and cisplatin in both cell lines (Table 1 and Fig. S1). GNS561 showed 100% inhibition of tumor cell proliferation at approximately 3 μM whereas gemcitabine did not reach total inhibition at the maximal tested concentration (15 μM for HuCCT1 and 6 μM for RBE).

We further determined whether GNS561-induced cancer cell death was related to caspase-dependent apoptosis in the two iCCA cell lines. After 8 h of exposure, GNS561 had little or no effect on caspases 3/7 activity and on cell viability in the two cell lines (Fig. 1a for HuCCT1 and Fig. 1b for RBE). In contrast, GNS561 induced caspases 3/7 activation after 24 h of treatment (Fig. 1c for HuCCT1 and Fig. 1d for RBE) and this activation was sustained at 30 h (Fig. 1e for HuCCT1 and Fig. 1f for RBE). This caspases activation was concomitant with a decrease in cell viability (Fig. 1).

Table 1 Mean IC_{50} ± SD of GNS561, gemcitabine and cisplatin in two human iCCA cell lines after 72 h of incubation

Cell lines	Mean IC_{50} ± SD (μM)		
	GNS561	Cisplatin	Gemcitabine
HuCCT1	1.5 ± 0.2	16.5 ± 0.5	75% max inhibition at 15 μM
RBE	1.7 ± 0.1	8.2 ± 1.2	60% max inhibition at 6 μM

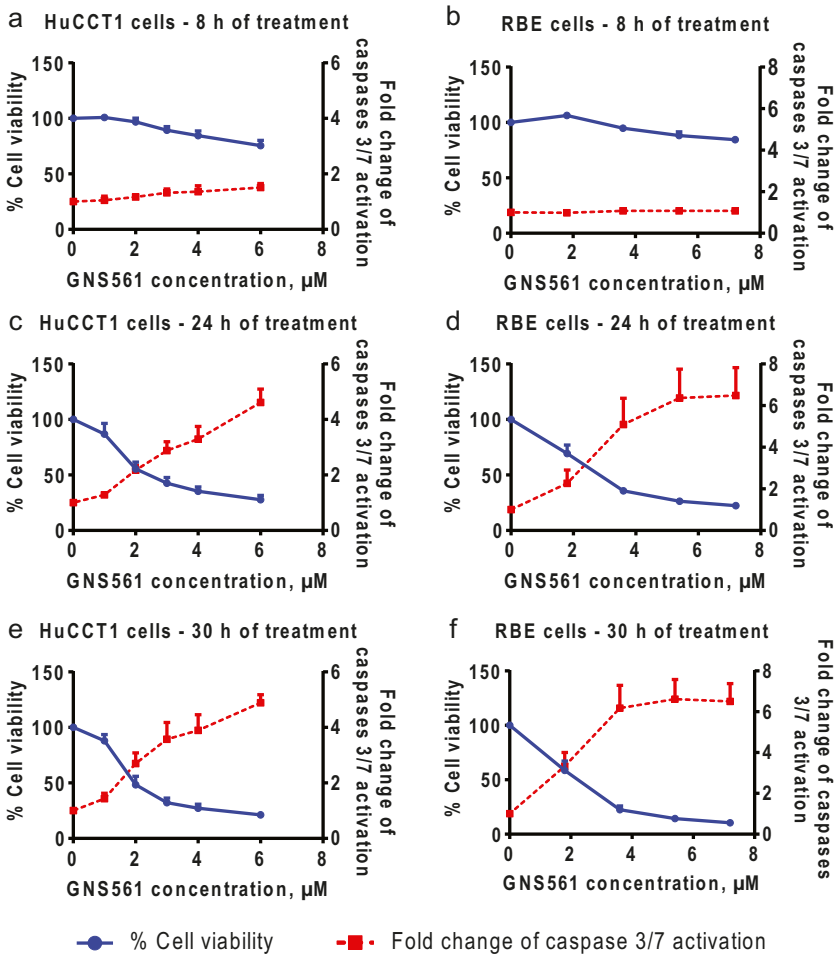

Fig. 1 Activation of caspases 3/7 by GNS561. Caspases 3/7 activation and cell viability of HuCCT1 (**a**, **c** and **e**) and RBE (**b**, **d** and **f**) cell lines after 8 h (**a** and **b**), 24 h (**c** and **d**) and 30 h (**e** and **f**) of treatment with GNS561 measured using the Caspase-Glo® 3/7 assay and CellTiter-Glo® viability assay. Data represent the mean + SD of three experiments

GNS561 induces cell death via its lysosomotropism

Since the concept of lysosomotropism was first introduced by Christian de Duve and his colleagues [57], it has been described that weakly basic lipophilic xenobiotics have a strong affinity for lysosomes. A weak base lipophilic drug is able to diffuse across the lysosomal membrane but cannot diffuse back to the cytosol as it becomes protonated when reaching the lysosome. A recent screening of lysosomotropic drugs found that drugs with a ClogP (partition coefficient of the neutral species of a compound between octanol and water, representing membrane permeability) above 2, and a pKa between 6.5 and 11, caused lysosomal accumulation [58]. Herein, the physicochemical characteristics of GNS561 showed weak base (pKa1 = 9.4, pKa2 = 7.6) and hydrophobic properties (logD = 2.52 at pH 7.4), which made it a drug with lysosomotropic properties.

Whether lysosomotropism is a contributor to cytotoxicity can be investigated by disrupting the lysosomal pH gradient either by inhibitors of the vacuolar (H+)-ATPase (Baf) or by treatment with NH_4Cl, which rapidly increases lysosomal pH [58, 59]. If Baf or NH_4Cl reduces the cytotoxicity caused by a lysosomotropic compound, this would suggest that lysosomotropism is a contributor to cell death. For this purpose, RBE cells were pretreated for 2 h by Baf or by NH_4Cl then treated with GNS561 for 24 h. Although concentrations of 100 and 200 nM Baf by themselves decreased viability (Fig. 2a), they significantly attenuated the still larger decrease in viability induced by GNS561. Pretreatment with NH_4Cl had the same protective effect (Fig. 2b). Therefore, disrupting the lysosomal pH gradient by either Baf or by NH_4Cl protected against GNS561-mediated cell death. These results suggested that GNS561-mediated cell death is caused by its lysosomotropic properties.

GNS561 inhibits late-stage autophagy and induces a dose-dependent build-up of enlarged lysosomes

The lysosomal-dependent cell death of GNS561 prompted us to examine its capacity to modulate autophagy that stands as a lysosomal-related pathway. We, therefore, examined the accumulation of LC3-II under GNS561 exposure. GNS561 induced a dose- and time-dependent accumulation of the LC3-II in the RBE cell line (Fig. 3a). Enhanced LC3-II levels can be associated either with an increased autophagosome synthesis or with a decreased autophagosome degradation as a result of delayed trafficking to the lysosomes, decreased fusion

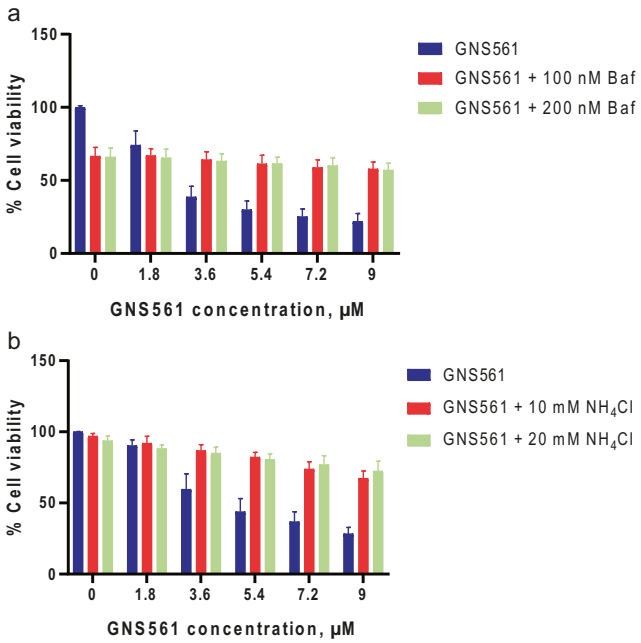

Fig. 2 GNS561-induced cell death due to its lysosomotropism. Cell viability (mean + SD) of RBE cells after 24 h of treatment with GNS561 in the presence or absence of Baf (**a**) or NH_4Cl (**b**) measured using CellTiter-Glo® viability assay

between compartments, and/or defective lysosomal proteolytic activity. To obtain a better evaluation of the autophagic flux, we carried out western blotting of control extracts harvested from cells treated with autophagy inhibitors, such as Baf, a specific vacuolar-type (H +)-ATPase inhibitor [60]. GNS561-induced accumulation of LC3-II was not enhanced in the presence of Baf (Fig. 3a), supporting the potential of GNS56l to inhibit degradation of the autophagic content.

As it was previously shown that lysosomotropic agents can increase the apparent steady-state volume of lysosomes in time- and concentration-dependent manners [28, 61–63], we focused on the structure of the lysosomes. Following continuous exposure to GNS561, LysoTracker staining was shown to increase (Fig. 3b and c) with an increase in total intensity and granule intensity values (Fig. 3b and c). From this experiment, it was concluded that GNS561 prompted a dose-dependent build-up of enlarged lysosomes.

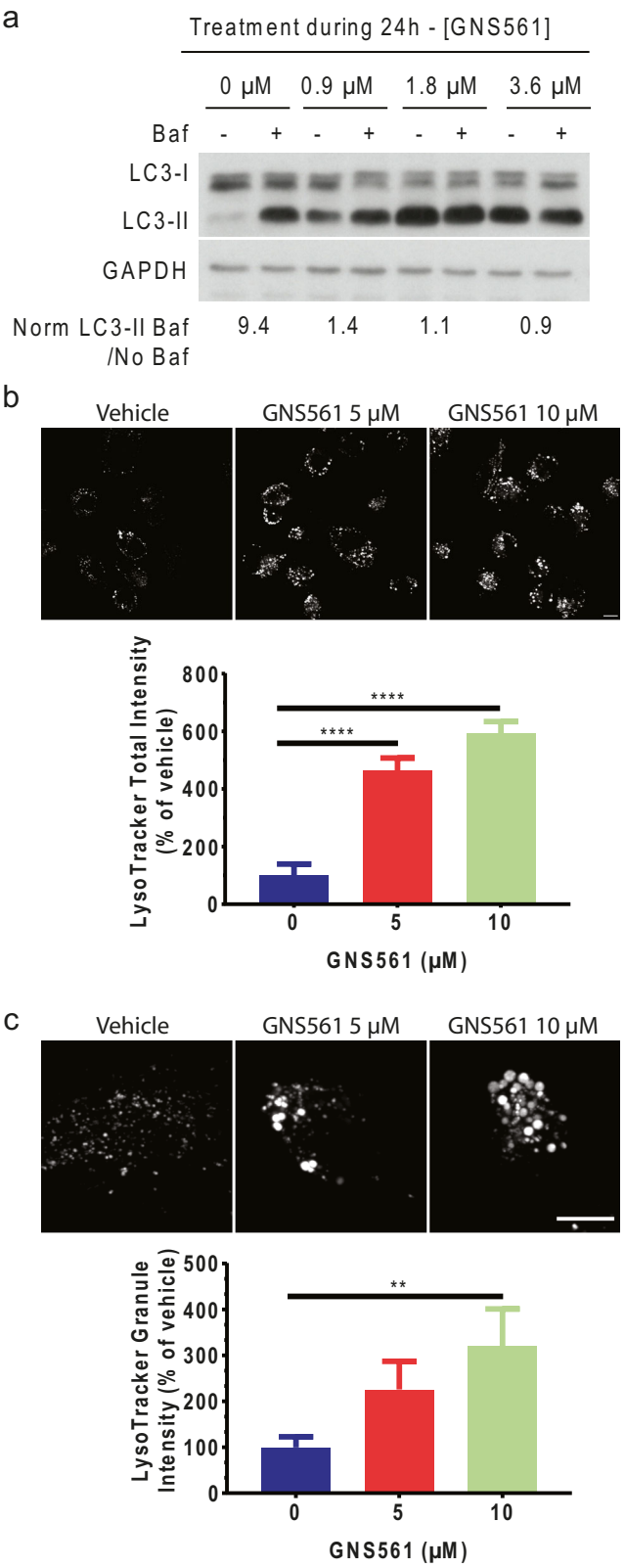

Fig. 3 Inhibition of the autophagy flux and induction enlarged lysosome build-up. a Immunoblot analysis of LC3-II levels were performed in RBE cell line incubated with vehicle (0 μM) or with indicated concentrations of GNS561 for 24 h in the presence or absence of Baf (100 nM, 2 h). GAPDH immunoblotting was used as a loading control. As indicated under each lane, the autophagic flux, determined as the ratio between the Norm LC3-II levels with Baf and without Baf, is expressed in arbitrary units. Three independent experiments were performed. A representative autoradiogram is shown. **b** and **c** RBE cells were treated with GNS561 at the indicated concentrations for 30 min. The medium was removed, and the LysoTracker probe was added. Three large microscopy images showing multiple cells (**b**, Scale bar, 10 μm) and three high-power photomicrographs showing one cell per field (**c**, Scale bar, 10 μm) were collected per condition. The total (**b**) or granule (**c**) intensities were measured using Metamorph software. Data represent the mean of three large images or of three single cell images per condition and were plotted as a percentage of vehicle + SD. *p*-values were calculated using Dunnett's multiple comparisons test

GNS561 is efficient against iCCA patient-derived cells

To further describe the activity of GNS561, we determined the antitumor activity of GNS561 on primary patient tumors in five iCCA patient-derived xenograft models using an ex vivo 3D methylcellulose assay. Each model was tested with GNS561 and two reference control drugs frequently used in iCCA (gemcitabine and cisplatin). The results indicated that GNS561 was more potent than cisplatin or gemcitabine in 2 models (CC6638 and CC6279, Fig. S2b and c, and CC6638 and CC6625, Fig. S2b and d, respectively). GNS561 was as effective as cisplatin in 3 out 5 iCCA patient-derived cell line models (CC6205, CC6625 and CC6658, Fig. S2a, d and e) and as gemcitabine in one model (CC6658, Fig. S2e). However, it is important to note that GNS561 always induced a complete tumor inhibition in all models, contrary to gemcitabine which did not in any model, suggesting that GNS561 may be efficient in models with low sensitivity to gemcitabine. Detailed IC_{50} values of GNS561, gemcitabine and cisplatin are shown in Table 2.

GNS561 is efficient in vivo against a human iCCA cell line in a chicken CAM xenograft model

Finally, we tested the effect of GNS561 on tumor growth in vivo by using the chick embryo model. HuCCT1 cells were grafted on the CAM and formed tumors were treated every 48 h with vehicle or GNS561 at two different doses (Fig. 4a). Gemcitabine was used as a positive control and a concentration of 150 μM was chosen to induce significant tumor growth inhibition without embryo toxicity. At day 18, we found that GNS561 significantly inhibited tumor growth compared with the vehicle treatment, even at the lowest concentration (Fig. 4b). Importantly, the comparison of the number of dead chicken embryos in the vehicle- and GNS561-treated eggs indicated that GNS561 showed no noticeable toxicity in the chicken embryo at all tested doses (Fig. 4c). This suggests that GNS561 is well tolerated, even at a high active concentration, in this model.

Discussion

The WHO classified liver cancers as devastating tumor types in terms of both incidence and mortality [1]; among them, iCCA is the second most common liver malignancy, following hepatocellular carcinoma. Drug pipelines for the treatment of advanced iCCA remain poor despite recent advances using targeted therapies that showed benefits in small subpopulations of iCCA patients [64]. In this context, we discovered and developed a new small agent, GNS561, with physicochemical properties that may be of interest for the treatment of patients with advanced iCCA. In vitro, we showed that GNS561 was more efficient than gemcitabine or cisplatin in two iCCA cell lines (11 and 4.8-fold more than cisplatin in HuCCT1 and RBE, respectively, and more than 3.5-fold greater than gemcitabine). This anticancer activity was confirmed in five different iCCA patient-derived cell lines. Moreover, in these models, GNS561 was potent in models with low sensitivity to gemcitabine. Ultimately, the GNS561 effect was assessed in an iCCA chicken CAM xenograft model. This model is of particular interest as it is considered a cost-effective and reliable alternative to the in vivo PDX model [65]. The highly vascularized nature of the CAM model greatly promotes the efficiency of tumor cell engraftment. Remarkably, within 8 days, HuCCT1 tumor cells developed sizable tumors. The tumors grown on the CAM of embryonated chicken eggs represent a fast, easy and affordable system for an initial preclinical analysis of the effects of a compound. In addition to demonstrating a significant antitumor activity in this iCCA chicken CAM xenograft model, GNS561 was also shown to be safe at active concentration levels.

Our findings suggest that GNS561 anticancer properties are dependent on its lysosomal affinity. Since caspase-dependent apoptosis is the best-known modality of programmed cell death, we first determined whether GNS561-induced cell death was due to apoptosis. Our study indicated that GNS561 induced caspase activation concomitantly with a decrease in cell viability. Abolition of GNS561 antitumor effects by disruption of the lysosomal pH gradient confirmed that lysosomotropism is responsible for GNS561-induced cell

Table 2 IC_{50} and maximal inhibition of GNS561, gemcitabine and cisplatin in five iCCA patient-derived models in ex vivo 3D methylcellulose assay after 7 days of incubation

Model name	GNS561		Gemcitabine		Cisplatin	
	IC_{50} (μM)	Maximal inhibition	IC_{50} (μM)	Maximal inhibition	IC_{50} (μM)	Maximal inhibition
CC6205	1.56	99.93%	0.026	86.3 7%	1.62	99.53%
CC6638	0.86	99.98%	> 10	49.16%	10.54	93.48%
CC6279	1.48	99.96%	0.010	83.73%	6.17	98.79%
CC6625	1.14	99.97%	13.61	52.57%	1.89	98.19%
CC6658	1.23	100.00%	0.53	89.98%	0.85	99.81%

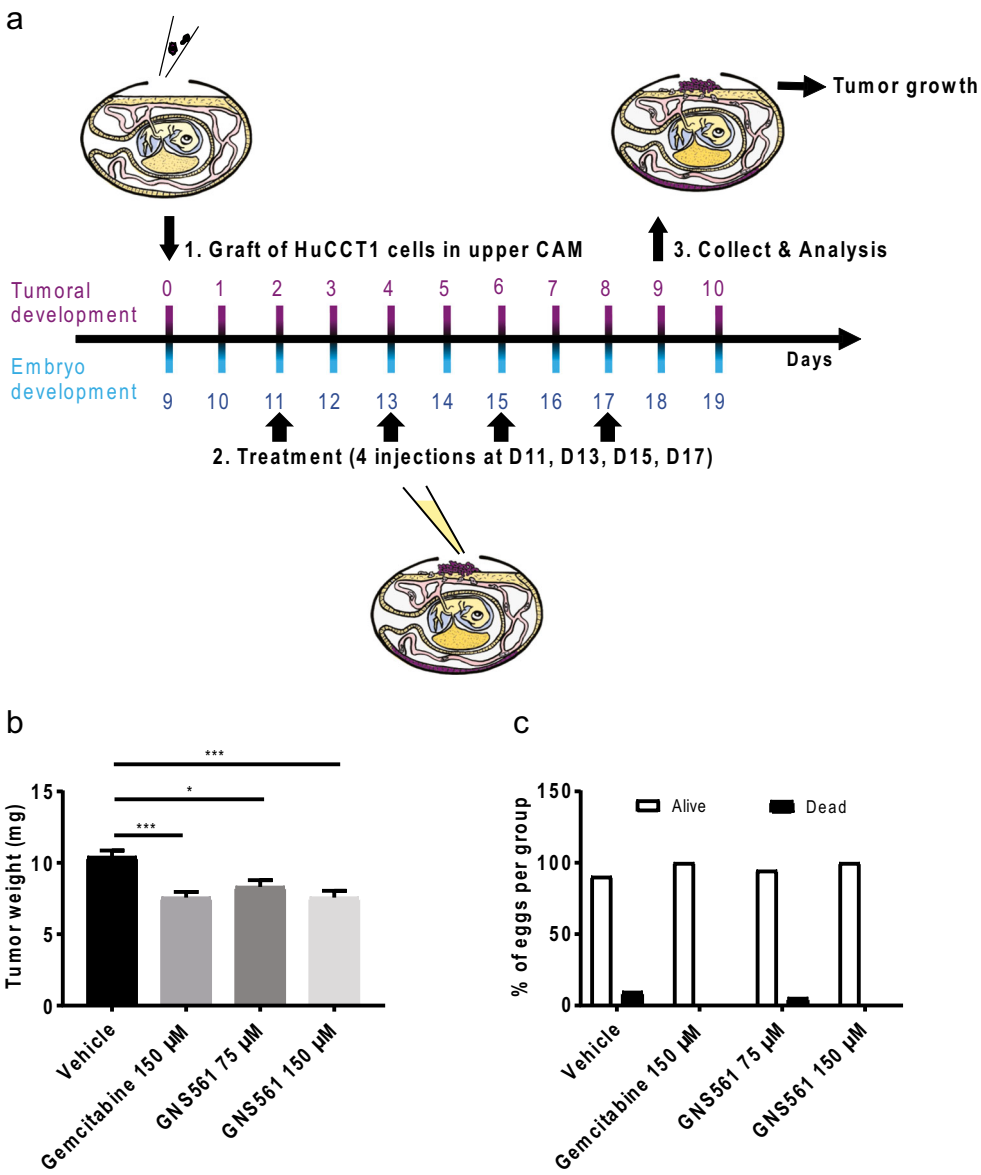

Fig. 4 GNS561 is efficient in vivo against human iCCA cell line HuCCT1 in a chicken CAM xenograft model. a Schematic representation of the assay principle, courtesy of Inovotion. **b** Effects of treatments on the HuCCT1 tumor weight (mean ± SEM of ≥ 18 samples) after 8 days of treatment. p-values were calculated using Dunn's multiple comparisons test. **c** Number of dead and surviving embryos for the different experimental groups after 8 days of treatment

death. Moreover, we showed that GNS561 induced a dose-dependent build-up of enlarged lysosomes. This observation was in agreement with previous studies regarding the capability of lysosomotropic agents to cause lysosomal stress and lysosomal enlargement [28, 61–63]. More investigations are needed to fully elucidate the cause of the GNS561-induced lysosomal volume expansion. We then demonstrated that GNS561 inhibited autophagic flux. This inhibition of the autophagic process is consistent with our observation of larger lysosomes. Indeed, it is well described that enlarged lysosomes present activity impairment leading to the accumulation of undegraded materials [63, 66, 67]. In addition, lysosomal swelling often precedes LMP [33, 38, 68]. Ono et al. suggested that enlargement of the lysosomes may alter the lysosomal membrane tension and, therefore, increase their susceptibility to rupture [33]. Since the surface tension is related to the lysosomal size, the larger lysosomes should be easier to breakdown.

Based on our results, we could hypothesize that GNS561 induces LMP and cathepsin release in the cytosol responsible for caspase activation and apoptotic cell death. In fact, it is known that once in the cytosol, cathepsins, particularly cysteine cathepsins B and L and aspartate cathepsin D, can initiate the apoptosis pathway by direct caspase activation [26, 36, 37, 69]. Similar to our findings, other groups already observed that several lysosomotropic compounds caused LMP [26, 67, 70, 71], suggesting that lysosomotropism in itself could contribute to cell death. Mechanisms may differ depending on chemical drug structures. For instance, for nonpermeable charged substances, their accumulation could build up an osmotic pressure across the lysosomal membrane, which results in the inflow of water that induces LMP [72, 73]. For other

lysosomotropic drugs, LMP is attributed to the inhibition of acid sphingomyelinase, a lysosomal enzyme that catalyzes the degradation of sphingomyelin to ceramide [12, 74, 75]. However, in most cases, mechanisms for LMP are lacking. Further research will be necessary to better understand these underlying mechanisms.

Several reports suggest that lysosomes in tumor cells are more fragile than normal lysosomes and are more susceptible to LMP [12, 14, 33, 34, 76]. Therefore, drugs that sensitize lysosomes and promote LMP, leading to cell death, may exert useful antitumor effects [76]. Most importantly, as cells with high metastatic properties are more susceptible to lysosome dysfunctions [23], agents inducing lysosomal-cell death may have strong a clinical benefit in the metastatic setting.

To our knowledge, this is the first supportive data highlighting lysosomes as a potential target to overcome tumor growth in iCCA. We showed that the anticancer activity of GNS561 was linked to lysosomal cell death. To date, no other lysosomotropic agent has shown the ability to induce cellular apoptosis in iCCA. Furthermore, GNS561 was capable of achieving more antitumor activity than gemcitabine, which stands as a gold standard for iCCA.

Altogether, these results support the use of GNS561 in iCCA treatment. Based on these findings, we obtained US FDA IND (Investigational New Drug) status and the EMA (European Medicine Agency) CTA (Clinical Trial Application) submitted in October 2017. GNS561 is also currently being assessed in advanced iCCA patients in an international clinical Phase 1b/2a study [77]. This was the first time that a lysosomotropic agent was investigated at clinical-stage for treatment of iCCA. Indeed, many other drugs with lysosomal tropism are currently being assessed in many cancers types, but none in the iCCA setting [22]. Ongoing clinical trials should confirm the safety and efficacy of GNS561 in primary liver cancers.

In summary, our data confirm the potent anticancer activity of GNS561, a new lysosomotropic agent, in iCCA. For the first time, we provide evidence that targeting lysosomes in iCCA exerts useful antitumor activity. This supports further development of lysosome-targeting compounds for iCCA therapy. Further studies are now required to investigate the underlying mechanism of action of GNS561 and to explore its anticancer activity in other types of cancer.

Acknowledgements The authors are very grateful to Dr. Emilien Dosda, Dr. Xavier Rousset and Sylvain Roveda from Inovotion for their work on the CAM study.

Funding This study was supported by private funding.

Compliance with ethical standards

Conflict of interest All authors declare that they have no conflict of interest and consent to the submission of this manuscript.

Ethical approval According to the French legislation, no ethical approval is needed for scientific experimentations using oviparous embryos (decree n° 2013–118, February 1, 2013; art. R-214–88).

Informed consent For this type of study, formal consent is not required. This article does not contain any studies with human participants or animals performed by any of the authors.

Publisher's note Springer Nature remains neutral with regard to jurisdictional claims in published maps and institutional affiliations.

References

1. World Health Organization (2018) Cancer. https://www.who.int/news-room/fact-sheets/detail/cancer. Accessed December 18, 2018
2. Kirstein MM, Vogel A (2016) Epidemiology and risk factors of cholangiocarcinoma. Visc Med 32(6):395–400. https://doi.org/10.1159/000453013
3. Valle J, Wasan H, Palmer DH, Cunningham D, Anthoney A, Maraveyas A, Madhusudan S, Iveson T, Hughes S, Pereira SP, Roughton M, Bridgewater J, Investigators ABCT (2010) Cisplatin plus gemcitabine versus gemcitabine for biliary tract cancer. N Engl J Med 362(14):1273–1281. https://doi.org/10.1056/NEJMoa0908721
4. El-Serag HB, Engels EA, Landgren O, Chiao E, Henderson L, Amaratunge HC, Giordano TP (2009) Risk of hepatobiliary and pancreatic cancers after hepatitis C virus infection: a population-based study of U.S. veterans. Hepatology 49(1):116–123. https://doi.org/10.1002/hep.22606
5. Ariizumi S, Yamamoto M (2015) Intrahepatic cholangiocarcinoma and cholangiolocellular carcinoma in cirrhosis and chronic viral hepatitis. Surg Today 45(6):682–687. https://doi.org/10.1007/s00595-014-1031-0
6. Razumilava N, Gores GJ (2014) Cholangiocarcinoma. Lancet 383(9935):2168–2179. https://doi.org/10.1016/S0140-6736(13)61903-0
7. Bridgewater J, Galle PR, Khan SA, Llovet JM, Park JW, Patel T, Pawlik TM, Gores GJ (2014) Guidelines for the diagnosis and management of intrahepatic cholangiocarcinoma. J Hepatol 60(6):1268–1289. https://doi.org/10.1016/j.jhep.2014.01.021
8. Lamarca A, Hubner RA, David Ryder W, Valle JW (2014) Second-line chemotherapy in advanced biliary cancer: a systematic review. Ann Oncol 25(12):2328–2338. https://doi.org/10.1093/annonc/mdu162
9. Walter T, Horgan AM, McNamara M, McKeever L, Min T, Hedley D, Serra S, Krzyzanowska MK, Chen E, Mackay H, Feld R, Moore M, Knox JJ (2013) Feasibility and benefits of second-line chemotherapy in advanced biliary tract cancer: a large retrospective study. Eur J Cancer 49(2):329–335. https://doi.org/10.1016/j.ejca.2012.08.003
10. Mahipal A, Kommalapati A, Tella SH, Lim A, Kim R (2018) Novel targeted treatment options for advanced cholangiocarcinoma. Expert Opin Investig Drugs 27(9):709–720. https://doi.org/10.1080/13543784.2018.1512581
11. Nakamura H, Arai Y, Totoki Y, Shirota T, Elzawahry A, Kato M, Hama N, Hosoda F, Urushidate T, Ohashi S, Hiraoka N, Ojima H, Shimada K, Okusaka T, Kosuge T, Miyagawa S, Shibata T (2015) Genomic spectra of biliary tract cancer. Nat Genet 47(9):1003–1010. https://doi.org/10.1038/ng.3375
12. Kallunki T, Olsen OD, Jaattela M (2013) Cancer-associated lysosomal changes: friends or foes? Oncogene 32(16):1995–2004. https://doi.org/10.1038/onc.2012.292

13. Perera RM, Stoykova S, Nicolay BN, Ross KN, Fitamant J, Boukhali M, Lengrand J, Deshpande V, Selig MK, Ferrone CR, Settleman J, Stephanopoulos G, Dyson NJ, Zoncu R, Ramaswamy S, Haas W, Bardeesy N (2015) Transcriptional control of autophagy-lysosome function drives pancreatic cancer metabolism. Nature 524(7565):361–365. https://doi.org/10.1038/nature14587
14. Appelqvist H, Waster P, Kagedal K, Ollinger K (2013) The lysosome: from waste bag to potential therapeutic target. J Mol Cell Biol 5(4):214–226. https://doi.org/10.1093/jmcb/mjt022
15. De Duve C, Pressman BC, Gianetto R, Wattiaux R, Appelmans F (1955) Tissue fractionation studies. 6. Intracellular distribution patterns of enzymes in rat-liver tissue. Biochem J 60(4):604–617
16. Xu H, Ren D (2015) Lysosomal physiology. Annu Rev Physiol 77: 57–80. https://doi.org/10.1146/annurev-physiol-021014-071649
17. de Duve C (1983) Lysosomes revisited. Eur J Biochem 137(3): 391–397
18. Boyer MJ, Tannock IF (1993) Lysosomes, lysosomal enzymes,. Adv Cancer Res 60:269–291
19. Kroemer G, Jaattela M (2005) Lysosomes and autophagy in cell death control. Nat Rev Cancer 5(11):886–897. https://doi.org/10.1038/nrc1738
20. Castino R, Demoz M, Isidoro C (2003) Destination 'lysosome': a target organelle for tumour cell killing? J Mol Recognit 16(5):337–348. https://doi.org/10.1002/jmr.643
21. Hamalisto S, Jaattela M (2016) Lysosomes in cancer-living on the edge (of the cell). Curr Opin Cell Biol 39:69–76. https://doi.org/10.1016/j.ceb.2016.02.009
22. Davidson SM, Vander Heiden MG (2017) Critical functions of the lysosome in Cancer biology. Annu Rev Pharmacol Toxicol 57:481–507. https://doi.org/10.1146/annurev-pharmtox-010715-103101
23. Morgan MJ, Fitzwalter BE, Owens CR, Powers RK, Sottnik JL, Gamez G, Costello JC, Theodorescu D, Thorburn A (2018) Metastatic cells are preferentially vulnerable to lysosomal inhibition. Proc Natl Acad Sci U S A 115(36):E8479–E8488. https://doi.org/10.1073/pnas.1706526115
24. Martinez-Carreres L, Nasrallah A, Fajas L (2017) Cancer: linking powerhouses to suicidal bags. Front Oncol 7:204. https://doi.org/10.3389/fonc.2017.00204
25. Saftig P, Sandhoff K (2013) Cancer: killing from the inside. Nature 502(7471):312–313. https://doi.org/10.1038/nature12692
26. Boya P, Kroemer G (2008) Lysosomal membrane permeabilization in cell death. Oncogene 27(50):6434–6451. https://doi.org/10.1038/onc.2008.310
27. Glunde K, Guggino SE, Solaiyappan M, Pathak AP, Ichikawa Y, Bhujwalla ZM (2003) Extracellular acidification alters lysosomal trafficking in human breast cancer cells. Neoplasia 5(6):533–545
28. Zhitomirsky B, Assaraf YG (2016) Lysosomes as mediators of drug resistance in cancer. Drug Resist Updat 24:23–33. https://doi.org/10.1016/j.drup.2015.11.004
29. Fehrenbacher N, Gyrd-Hansen M, Poulsen B, Felbor U, Kallunki T, Boes M, Weber E, Leist M, Jaattela M (2004) Sensitization to the lysosomal cell death pathway upon immortalization and transformation. Cancer Res 64(15):5301–5310. https://doi.org/10.1158/0008-5472.CAN-04-1427
30. Domagala A, Fidyt K, Bobrowicz M, Stachura J, Szczygiel K, Firczuk M (2018) Typical and atypical inducers of lysosomal cell death: a promising anticancer strategy. Int J Mol Sci 19(8). https://doi.org/10.3390/ijms19082256
31. Fennelly C, Amaravadi RK (2017) Lysosomal biology in cancer. Methods Mol Biol 1594:293–308. https://doi.org/10.1007/978-1-4939-6934-0_19
32. Kirkegaard T, Jaattela M (2009) Lysosomal involvement in cell death and cancer. Biochim Biophys Acta 1793(4):746–754. https://doi.org/10.1016/j.bbamcr.2008.09.008
33. Ono K, Kim SO, Han J (2003) Susceptibility of lysosomes to rupture is a determinant for plasma membrane disruption in tumor necrosis factor alpha-induced cell death. Mol Cell Biol 23(2): 665–676
34. Petersen NH, Olsen OD, Groth-Pedersen L, Ellegaard AM, Bilgin M, Redmer S, Ostenfeld MS, Ulanet D, Dovmark TH, Lonborg A, Vindelov SD, Hanahan D, Arenz C, Ejsing CS, Kirkegaard T, Rohde M, Nylandsted J, Jaattela M (2013) Transformation-associated changes in sphingolipid metabolism sensitize cells to lysosomal cell death induced by inhibitors of acid sphingomyelinase. Cancer Cell 24(3):379–393. https://doi.org/10.1016/j.ccr.2013.08.003
35. Piao S, Amaravadi RK (2016) Targeting the lysosome in cancer. Ann N Y Acad Sci 1371(1):45–54. https://doi.org/10.1111/nyas.12953
36. Serrano-Puebla A, Boya P (2018) Lysosomal membrane permeabilization as a cell death mechanism in cancer cells. Biochem Soc Trans 46(2):207–215. https://doi.org/10.1042/BST20170130
37. Wang F, Gomez-Sintes R, Boya P (2018) Lysosomal membrane permeabilization and cell death. Traffic 19(12):918–931. https://doi.org/10.1111/tra.12613
38. Halaby R (2015) Role of lysosomes in cancer therapy. Res Rep Biol 6:147–155. https://doi.org/10.2147/RRB.S83999
39. Hou YJ, Dong LW, Tan YX, Yang GZ, Pan YF, Li Z, Tang L, Wang M, Wang Q, Wang HY (2011) Inhibition of active autophagy induces apoptosis and increases chemosensitivity in cholangiocarcinoma. Lab Investig 91(8):1146–1157. https://doi.org/10.1038/labinvest.2011.97
40. Nitta T, Sato Y, Ren XS, Harada K, Sasaki M, Hirano S, Nakanuma Y (2014) Autophagy may promote carcinoma cell invasion and correlate with poor prognosis in cholangiocarcinoma. Int J Clin Exp Pathol 7(8):4913–4921
41. Thongchot S, Yongvanit P, Loilome W, Seubwai W, Phunicom K, Tassaneeyakul W, Pairojkul C, Promkotra W, Techasen A, Namwat N (2014) High expression of HIF-1alpha, BNIP3 and PI3KC3: hypoxia-induced autophagy predicts cholangiocarcinoma survival and metastasis. Asian Pac J Cancer Prev 15(14):5873–5878
42. Sasaki M, Nitta T, Sato Y, Nakanuma Y (2015) Autophagy may occur at an early stage of cholangiocarcinogenesis via biliary intraepithelial neoplasia. Hum Pathol 46(2):202–209. https://doi.org/10.1016/j.humpath.2014.09.016
43. Boya P, Gonzalez-Polo RA, Poncet D, Andreau K, Vieira HL, Roumier T, Perfettini JL, Kroemer G (2003) Mitochondrial membrane permeabilization is a critical step of lysosome-initiated apoptosis induced by hydroxychloroquine. Oncogene 22(25):3927–3936. https://doi.org/10.1038/sj.onc.1206622
44. Zhang Y, Liao Z, Zhang LJ, Xiao HT (2015) The utility of chloroquine in cancer therapy. Curr Med Res Opin 31(5):1009–1013. https://doi.org/10.1185/03007995.2015.1025731
45. Fu W, Li X, Lu X, Zhang L, Li R, Zhang N, Liu S, Yang X, Wang Y, Zhao Y, Meng X, Zhu WG (2017) A novel acridine derivative, LS-1-10 inhibits autophagic degradation and triggers apoptosis in colon cancer cells. Cell Death Dis 8(10):e3086. https://doi.org/10.1038/cddis.2017.498
46. Xu R, Ji Z, Xu C, Zhu J (2018) The clinical value of using chloroquine or hydroxychloroquine as autophagy inhibitors in the treatment of cancers: a systematic review and meta-analysis. Medicine (Baltimore) 97(46):e12912. https://doi.org/10.1097/MD.0000000000012912
47. Rebecca VW, Amaravadi RK (2016) Emerging strategies to effectively target autophagy in cancer. Oncogene 35(1):1–11. https://doi.org/10.1038/onc.2015.99
48. Manic G, Obrist F, Kroemer G, Vitale I, Galluzzi L (2014) Chloroquine and hydroxychloroquine for cancer therapy. Mol Cell Oncol 1(1):e29911. https://doi.org/10.4161/mco.29911
49. Verbaanderd C, Maes H, Schaaf MB, Sukhatme VP, Pantziarka P, Sukhatme V, Agostinis P, Bouche G (2017) Repurposing drugs in oncology (ReDO)-chloroquine and hydroxychloroquine as anti-

cancer agents. Ecancermedicalscience 11:781. https://doi.org/10.3332/ecancer.2017.781
50. Plantone D, Koudriavtseva T (2018) Current and future use of chloroquine and hydroxychloroquine in infectious, immune, neoplastic, and neurological diseases: a mini-review. Clin Drug Investig 38(8):653–671. https://doi.org/10.1007/s40261-018-0656-y
51. Pascolo S (2016) Time to use a dose of chloroquine as an adjuvant to anti-cancer chemotherapies. Eur J Pharmacol 771:139–144. https://doi.org/10.1016/j.ejphar.2015.12.017
52. Bernstein HN (1991) Ocular safety of hydroxychloroquine. Ann Ophthalmol 23(8):292–296
53. Prudent R, Vassal-Stermann E, Nguyen CH, Mollaret M, Viallet J, Desroches-Castan A, Martinez A, Barette C, Pillet C, Valdameri G, Soleilhac E, Di Pietro A, Feige JJ, Billaud M, Florent JC, Lafanechere L (2013) Azaindole derivatives are inhibitors of microtubule dynamics, with anti-cancer and anti-angiogenic activities. Br J Pharmacol 168(3):673–685. https://doi.org/10.1111/j.1476-5381.2012.02230.x
54. Al Dhaheri Y, Attoub S, Arafat K, Abuqamar S, Viallet J, Saleh A, Al Agha H, Eid A, Iratni R (2013) Anti-metastatic and anti-tumor growth effects of Origanum majorana on highly metastatic human breast cancer cells: inhibition of NFkappaB signaling and reduction of nitric oxide production. PLoS One 8(7):e68808. https://doi.org/10.1371/journal.pone.0068808
55. El Hasasna H, Saleh A, Al Samri H, Athamneh K, Attoub S, Arafat K, Benhalilou N, Alyan S, Viallet J, Al Dhaheri Y, Eid A, Iratni R (2016) Rhus coriaria suppresses angiogenesis, metastasis and tumor growth of breast cancer through inhibition of STAT3, NFkappaB and nitric oxide pathways. Sci Rep 6:21144. https://doi.org/10.1038/srep21144
56. Gilson P, Josa-Prado F, Beauvineau C, Naud-Martin D, Vanwonterghem L, Mahuteau-Betzer F, Moreno A, Falson P, Lafanechere L, Frachet V, Coll JL, Fernando Diaz J, Hurbin A, Busser B (2017) Identification of pyrrolopyrimidine derivative PP-13 as a novel microtubule-destabilizing agent with promising anticancer properties. Sci Rep 7(1):10209. https://doi.org/10.1038/s41598-017-09491-9
57. de Duve C, de Barsy T, Poole B, Trouet A, Tulkens P, Van Hoof F (1974) Commentary. Lysosomotropic agents. Biochem Pharmacol 23(18):2495–2531
58. Nadanaciva S, Lu S, Gebhard DF, Jessen BA, Pennie WD, Will Y (2011) A high content screening assay for identifying lysosomotropic compounds. Toxicol in Vitro 25(3):715–723. https://doi.org/10.1016/j.tiv.2010.12.010
59. Yoshimori T, Yamamoto A, Moriyama Y, Futai M, Tashiro Y (1991) Bafilomycin A1, a specific inhibitor of vacuolar-type H(+)-ATPase, inhibits acidification and protein degradation in lysosomes of cultured cells. J Biol Chem 266(26):17707–17712
60. Klionsky DJ, Abdelmohsen K, Abe A et al (2016) Guidelines for the use and interpretation of assays for monitoring autophagy (3rd edition). Autophagy 12 (1):1–222. https://doi.org/10.1080/15548627.2015.1100356
61. Logan R, Kong AC, Axcell E, Krise JP (2014) Amine-containing molecules and the induction of an expanded lysosomal volume phenotype: a structure-activity relationship study. J Pharm Sci 103(5):1572–1580. https://doi.org/10.1002/jps.23949
62. Logan R, Kong AC, Krise JP (2014) Time-dependent effects of hydrophobic amine-containing drugs on lysosome structure and biogenesis in cultured human fibroblasts. J Pharm Sci 103(10):3287–3296. https://doi.org/10.1002/jps.24087
63. Lu S, Sung T, Lin N, Abraham RT, Jessen BA (2017) Lysosomal adaptation: how cells respond to lysosomotropic compounds. PLoS One 12(3):e0173771. https://doi.org/10.1371/journal.pone.0173771
64. Ventola CL (2017) Cancer immunotherapy, part 3: challenges and future trends. P T 42(8):514–521
65. DeBord LC, Pathak RR, Villaneuva M, Liu HC, Harrington DA, Yu W, Lewis MT, Sikora AG (2018) The chick chorioallantoic membrane (CAM) as a versatile patient-derived xenograft (PDX) platform for precision medicine and preclinical research. Am J Cancer Res 8(8):1642–1660
66. Repnik U, Borg Distefano M, Speth MT, Ng MYW, Progida C, Hoflack B, Gruenberg J, Griffiths G (2017) L-leucyl-L-leucine methyl ester does not release cysteine cathepsins to the cytosol but inactivates them in transiently permeabilized lysosomes. J Cell Sci 130(18):3124–3140. https://doi.org/10.1242/jcs.204529
67. Ashoor R, Yafawi R, Jessen B, Lu S (2013) The contribution of lysosomotropism to autophagy perturbation. PLoS One 8(11):e82481. https://doi.org/10.1371/journal.pone.0082481
68. Hsu SPC, Kuo JS, Chiang HC, Wang HE, Wang YS, Huang CC, Huang YC, Chi MS, Mehta MP, Chi KH (2018) Temozolomide, sirolimus and chloroquine is a new therapeutic combination that synergizes to disrupt lysosomal function and cholesterol homeostasis in GBM cells. Oncotarget 9(6):6883–6896. https://doi.org/10.18632/oncotarget.23855
69. Chwieralski CE, Welte T, Buhling F (2006) Cathepsin-regulated apoptosis. Apoptosis 11(2):143–149. https://doi.org/10.1007/s10495-006-3486-y
70. Repnik U, Hafner Cesen M, Turk B (2014) Lysosomal membrane permeabilization in cell death: concepts and challenges. Mitochondrion 19 Pt A:49–57. https://doi.org/10.1016/j.mito.2014.06.006
71. Aits S, Jaattela M (2013) Lysosomal cell death at a glance. J Cell Sci 126(Pt9):1905–1912. https://doi.org/10.1242/jcs.091181
72. Uchimoto T, Nohara H, Kamehara R, Iwamura M, Watanabe N, Kobayashi Y (1999) Mechanism of apoptosis induced by a lysosomotropic agent, L-Leucyl-L-Leucine methyl ester. Apoptosis 4(5):357–362
73. Thiele DL, Lipsky PE (1990) Mechanism of L-leucyl-L-leucine methyl ester-mediated killing of cytotoxic lymphocytes: dependence on a lysosomal thiol protease, dipeptidyl peptidase I, that is enriched in these cells. Proc Natl Acad Sci U S A 87(1):83–87
74. Kornhuber J, Tripal P, Reichel M, Terfloth L, Bleich S, Wiltfang J, Gulbins E (2008) Identification of new functional inhibitors of acid sphingomyelinase using a structure-property-activity relation model. J Med Chem 51(2):219–237. https://doi.org/10.1021/jm070524a
75. Villamil Giraldo AM, Appelqvist H, Ederth T, Ollinger K (2014) Lysosomotropic agents: impact on lysosomal membrane permeabilization and cell death. Biochem Soc Trans 42(5):1460–1464. https://doi.org/10.1042/BST20140145
76. Fehrenbacher N, Bastholm L, Kirkegaard-Sorensen T, Rafn B, Bottzauw T, Nielsen C, Weber E, Shirasawa S, Kallunki T, Jaattela M (2008) Sensitization to the lysosomal cell death pathway by oncogene-induced down-regulation of lysosome-associated membrane proteins 1 and 2. Cancer Res 68(16):6623–6633. https://doi.org/10.1158/0008-5472.CAN-08-0463
77. ClinicalTrials.gov (2018) Study of GNS561 in Patients with liver cancer - full text view - ClinicalTrials.gov. https://clinicaltrials.gov/ct2/show/NCT03316222. Accessed December 18, 2018